

Construction, DNA wrapping and cleavage of a carbon nanotube–polypseudorotaxane conjugate†

Yong Chen,^a Lu Yu,^a Xi-Zeng Feng,^b Sen Hou^b and Yu Liu^{*a}

Received (in Cambridge, UK) 3rd April 2009, Accepted 11th May 2009

First published as an Advance Article on the web 8th June 2009

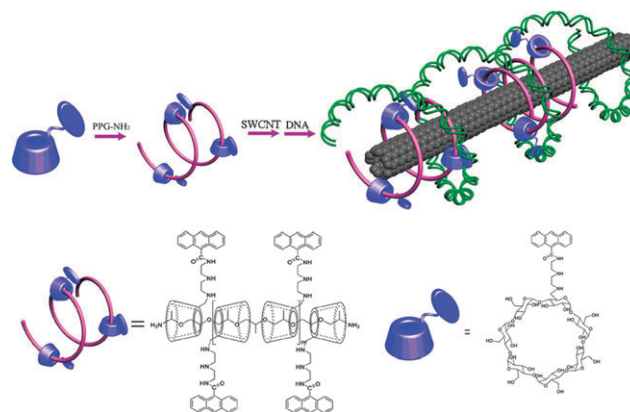
DOI: 10.1039/b906794a

A supramolecular assembly of carbon nanotubes was constructed by non-covalently wrapping cyclodextrin-based polypseudorotaxanes on single wall carbon nanotubes; the assembly showed good abilities in wrapping and cleaving double-stranded DNA.

The biological applications of single wall carbon nanotubes (SWCNTs) have attracted more and more interest over the past few years.^{1,2} Among them, DNA-wrapped SWCNTs have been widely investigated by experimental and simulative methods owing to their potential applications in gene delivery and gene therapy.^{3–12} Because the surface of a SWCNT is hydrophobic, it can be readily wrapped around by single-stranded DNA through hydrophobic and π - π stacking interactions, while it hardly interacts with double-stranded DNA in which the hydrophilic sites (phosphates) are exposed on the surface. Therefore, most of the studies of DNA–SWCNT conjugates are focused on the wrapping of single-stranded DNA,^{6–10} but corresponding research on the wrapping of double-stranded DNA is still rare.¹¹ It is well known that there are two methods to achieve the modification of SWCNTs, namely covalent and non-covalent modification of carbon nanotubes. Superior to the covalent approach, the non-covalent approach does not change the original structure and properties of the nanotubes, such as the physical, optical, electrical and mechanical properties. In this communication we show the wrapping of a double-stranded DNA onto SWCNTs assisted by the anthrylcyclodextrin-based polypseudorotaxane (ACD-PPR, Scheme 1). Significantly, the SWCNT–ACD-PPR conjugate is able to cleave DNA under visible light irradiation. There is an inherent advantage in using ACD-PPR as a medium to combine DNA and SWCNT, because cyclodextrins can be well adsorbed onto the SWCNTs¹³ and the anthryl group is capable of intercalating into the DNA grooves.¹⁴ The structure and morphology of the SWCNT–ACD-PPR conjugate and its DNA-associated species were characterized by UV-Vis, circular dichroism and fluorescence spectroscopies, atomic force microscopy (AFM), and transmission electron microscopy (TEM).

SWCNT–ACD-PPR conjugate was prepared in 58% yield by grinding a mixture of ACD-PPR¹⁵ and SWCNT followed by centrifugation and dialysis to remove the unreacted SWCNT and ACD-PPR, respectively. The UV-Vis spectrum of the SWCNT–ACD-PPR conjugate (see Fig. S1 in the ESI†) resembled that of free ACD-PPR, showing three absorbance maximums and a shoulder at 330, 346, 363 and 383 nm, respectively. It also showed an obvious upward shift of the baseline in the range of 500–1300 nm, attributed to the Rayleigh scattering of SWCNTs.¹⁶ Moreover, the fluorescence intensity of ACD-PPR showed a significant decrease after reacting with SWCNT (Fig. S1†), like the reported phenomena for SWCNT-pyrene¹⁷ and SWCNT-fluorescein¹⁸ systems. These results jointly indicated the association of ACD-PPR with SWCNT.

Owing to the ACD-PPR units associated to the SWCNTs, the resultant SWCNT–ACD-PPR conjugate exhibited a good ability in interacting with DNA, which could be readily observed through the circular dichroism and fluorescence spectroscopic studies. The circular dichroism spectrum of ct-DNA displayed a positive peak at *ca.* 275 nm and a negative peak at *ca.* 246 nm assigned to B-type DNA.¹⁹ With the addition of SWCNT–ACD-PPR conjugate at a relatively low concentration (see Fig. S2 in the ESI, lines b and c†), the circular dichroism signal of ct-DNA retained its original shape but the intensity decreased, indicating the decrease of B-type DNA.¹⁹ On further increasing the concentration of the SWCNT–ACD-PPR conjugate (Fig. S2, lines d and e†), the circular dichroism signal of ct-DNA showed a significant change, displaying only a negative peak at *ca.* 253 nm. This might suggest a large conformational change of ct-DNA induced by the SWCNT–ACD-PPR conjugate. In the control



Scheme 1 Preparation of a SWCNT–ACD-PPR conjugate and its DNA wrapping.

^a Department of Chemistry, State Key Laboratory of Elemento-Organic Chemistry, Nankai University, Tianjin 300071, P. R. China. E-mail: yuliu@nankai.edu.cn; Fax: +86 22 2350 3625; Tel: +86 22 2350 3625

^b College of Life Science, Nankai University, Tianjin 300071, P. R. China

† Electronic supplementary information (ESI) available: Experimental details; UV-Vis, fluorescence and circular dichroism spectra; plot of $\log K_s$ versus $1/T$; thermodynamic parameters. See DOI: 10.1039/b906794a

experiment, SWCNT-ACD-PPR conjugate showed no appreciable circular dichroism signals in the measured wavelength range.

For a qualitative assessment of the interactions between the SWCNT-ACD-PPR conjugate and ct-DNA, fluorescence titration experiments were also performed. In the fluorescence curves, the fluorescence intensity of the SWCNT-ACD-PPR conjugate around 411 nm gradually increased upon the addition of varying amounts of ct-DNA (see Fig. S3 in the ESI†). The increasing fluorescence may be attributed to the intercalation of anthryl groups in the SWCNT-ACD-PPR conjugate into the hydrophobic DNA grooves without energy transfer, because the singlet energies of the DNA bases were larger than that of the anthryl group by at least 15 kcal mol⁻¹.¹⁵ By analyzing the sequential changes of the fluorescence intensity (ΔF) of the SWCNT-ACD-PPR conjugate at 411 nm that occurred with changes in the DNA concentration using a nonlinear least-squares curve-fitting method, we could calculate the effective binding constant of every anthryl-modified β -cyclodextrin inclusion unit in the SWCNT-ACD-PPR conjugate (one ACD-PPR could be divided into *ca.* 9 anthryl-modified β -cyclodextrin inclusion units) with ct-DNA to be $1.70 \times 10^4 \text{ M}^{-1}$, after taking into account the influence of scattering,¹⁵ which is lower than that of ACD-PPR ($3.99 \times 10^4 \text{ M}^{-1}$) with DNA.

Temperature-dependent fluorescence titration experiments gave the thermodynamic parameters for interactions between the SWCNT-ACD-PPR conjugate and ct-DNA. The results showed that the association of ACD-PPR with ct-DNA gives rise to negative enthalpic changes ($\Delta H^\circ = -23.6 \text{ kJ mol}^{-1}$), accompanied by positive entropic changes ($T\Delta S^\circ = 2.7 \text{ kJ mol}^{-1}$). This may indicate that van der Waals and hydrophobic interactions are the main driving forces of the associations, because these two interactions between host and guest mainly contributed to the enthalpic changes. Further comparison showed that the binding of the SWCNT-ACD-PPR conjugate with ct-DNA gave a more favorable enthalpic contribution and a larger entropic loss than the binding of parent ACD-PPR with ct-DNA ($\Delta H^\circ = -29.6 \text{ kJ mol}^{-1}$, $T\Delta S^\circ = -5.4 \text{ kJ mol}^{-1}$). This result should be reasonable, because the introduction of SWCNT greatly enhanced the hydrophobicity of ACD-PPR, which consequently led to stronger hydrophobic interactions between host and guest. On the other hand, the association with SWCNT froze the conformation of DNA to a great degree. This process resulted in a large loss of conformational freedom, which was inherently accompanied by unfavorable entropic changes.

Direct information about the morphology of the SWCNT-ACD-PPR conjugate and its DNA-wrapped species came from microscopic experiments. Fig. 1 shows typical AFM images of the SWCNT-ACD-PPR conjugate in the absence and presence of ct-DNA on a mica substrate. As seen in Fig. 1a, SWCNTs were well dispersed after association with ACD-PPR. Moreover, the average length of the SWCNT-ACD-PPR conjugate (*ca.* 0.45 μm) was shorter than that of the naked SWCNT ($> 5 \mu\text{m}$), attributed to the cutting effect of ACD-PPR on SWCNT through the grinding and sonication.^{13a} Interestingly, the height of the SWCNT-ACD-PPR conjugate was measured to be *ca.* 3.1 nm,

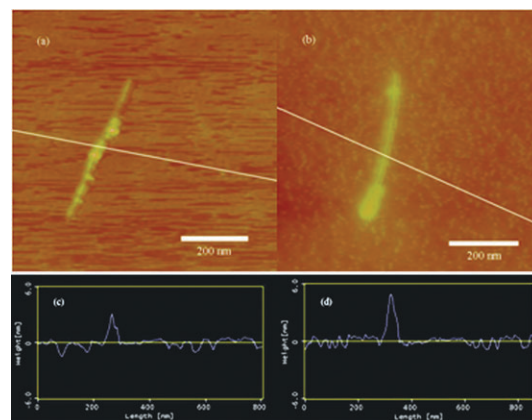


Fig. 1 AFM images of SWCNT-ACD-PPR conjugate ($1 \text{ ng } \mu\text{L}^{-1}$) in the absence (a) and the presence (b) of ct-DNA ($1 \text{ ng } \mu\text{L}^{-1}$) on mica in tapping mode; height profile of SWCNT-ACD-PPR conjugate in the absence (c) and the presence (d) of ct-DNA, respectively along lines in (a) and (b).

which was basically equal to the sum of the average diameter of naked SWCNTs (*ca.* 1.3–1.5 nm)²⁰ and the outer diameter of β -cyclodextrin (*ca.* 1.54 nm).²¹ This observation indicated that the ACD-PPRs were wrapped on the surfaces of the SWCNTs. After the ct-DNA was added, the SWCNT-ACD-PPR conjugate retained its original length but was obviously broadened (Fig. 1b). The measured height (*ca.* 5.0 nm) of the SWCNT-ACD-PPR conjugate in the presence of ct-DNA was 1.9 nm higher than that of the SWCNT-ACD-PPR conjugate itself (*ca.* 3.1 nm). This phenomenon may indicate that the ct-DNA was further wrapped on the SWCNT-ACD-PPR conjugate, and the height difference of 1.9 nm indicated that several DNA duplexes may wrap onto SWCNT-ACD-PPR rather than only one because the DNA duplex would dehydrate and has an apparent diameter of *ca.* 0.4 nm under the AFM air-tapping mode. In contrast, ACD-PPR showed a good ability to condense the free ct-DNA (existing as loose strands) to compacted solid particles without SWCNT, which was described in our preliminary report.¹⁵

TEM images further validated the different morphologies of DNA-ACD-PPR and DNA-SWCNT-ACD-PPR systems. Fig. 2a shows a typical high-resolution TEM image of the SWCNT-ACD-PPR conjugate, where the SWCNTs were found to be partly wrapped by ACD-PPR. After the addition of DNA, most of the SWCNT surface was covered, accompanied by the clear broadening of the nanotube (Fig. 2b). These results jointly confirmed that the ct-DNA was wrapped on the SWCNT-ACD-PPR conjugate. In the

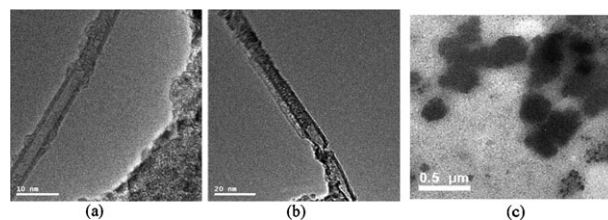


Fig. 2 High-resolution TEM images of (a) SWCNT-ACD-PPR, (b) DNA-SWCNT-ACD-PPR and (c) DNA-ACD-PPR systems.

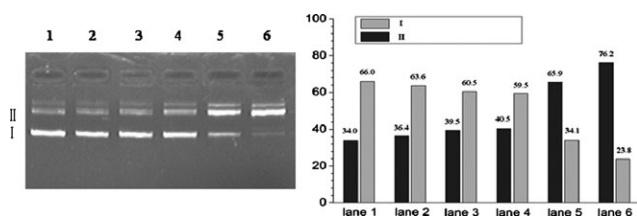


Fig. 3 Agarose gel electrophoresis assay of plasmid pEGFP-C2 DNA ($15 \text{ ng } \mu\text{L}^{-1}$ in $1 \text{ mM EDTA} - 10 \text{ mM Tris}$ buffer, $\text{pH } 8.0$) in the presence of SWCNT-ACD-PPR conjugate. ([SWCNT-ACD-PPR] = $0, 5, 25, 50, 250, 500 \text{ ng } \mu\text{L}^{-1}$ from lane 1 to 6). All the samples were incubated under visible light for 1 h.

control experiment, the naked SWCNTs were not dispersed in the presence of DNA in solution. In contrast, the TEM image of DNA-ACD-PPR showed a number of solid particles with diameters of *ca.* 200–300 nm.

Besides acting as a DNA carrier, the SWCNT-ACD-PPR conjugate also exhibited a good ability to cleave DNA. Fig. 3 illustrates an agarose gel electrophoresis assay of pEGFP-C2 DNA at various SWCNT-ACD-PPR concentrations. As seen in lane 1, there were two different forms of parent pEGFP-C2 DNA, namely closed supercoiled DNA (form I) and nicked circular DNA (form II). The SWCNT-ACD-PPR conjugate showed little to high DNA-cleavage activity with increasing SWCNT-ACD-PPR concentration. The percentage of nicked circular DNA increased slowly from 34.0% to 40.5% when the SWCNT-ACD-PPR concentration was below $50 \text{ ng } \mu\text{L}^{-1}$ (lanes 1–4), but increased rapidly from 65.9% to 76.2% on further increasing the SWCNT-ACD-PPR concentration from 250 to $500 \text{ ng } \mu\text{L}^{-1}$ (lanes 5 and 6). In the control experiment, ACD-PPR showed no appreciable cleavage activity under the same conditions. In a preliminary study, we have reported the photoinduced DNA-cleavage mechanism for cyclodextrin-fullerene conjugates.²² In this case, a singlet oxygen mechanism should be responsible for the DNA cleavage reaction. That is, the fullerene moiety in the conjugate was located close to the guanosine position of the DNA. Under visible-light irradiation, the singlet oxygen ($^1\text{O}_2$) was sensitized by the photoexcitation of fullerene. Then, the sensitized singlet oxygen reacted with the guanosines of DNA by either [4 + 2] or [2 + 2] cycloaddition to the five-membered imidazole ring of the purine base and thus cleaved the DNA. Because fullerenes and carbon nanotubes are congeners, we deduce that the DNA-cleavage mechanism for SWCNT-ACD-PPR should be similar to that for cyclodextrin-fullerene conjugates.

In conclusion, we have successfully developed an approach to wrap double-stranded DNA onto SWCNTs. During this process, an anthrylcyclodextrin-based polypseudorotaxane was used as a medium owing to its ability to wrap SWCNTs and interact with DNA; the wrapping process was driven by an exothermic enthalpic change. Significantly, the

SWCNT-ACD-PPR conjugate exhibited a good capability for DNA cleavage. These fascinating findings could provide new access to potential applications of nanotube-based supramolecular systems in many fields of chemistry and biology.

This work was supported financially by the 973 Program (2006CB932900), NNSFC (No. 20721062 and 20772062), and Tianjin Natural Science Foundation (07QTPTJC29600).

Notes and references

- 1 K. A. Williams, P. T. M. Veenhuizen, B. G. Torre, R. Eritja and C. Dekker, *Nature*, 2002, **420**, 761–762.
- 2 D. Tasis, N. Tagmatarchis, A. Bianco and M. Prato, *Chem. Rev.*, 2006, **106**, 1105–1136.
- 3 R. Singh, D. Pantarotto, D. McCarthy, O. Chaloin, J. Hoebeke, C. D. Partidos, J. P. Briand, M. Prato, A. Bianco and K. Kostarelos, *J. Am. Chem. Soc.*, 2005, **127**, 4388–4396.
- 4 D. Pantarotto, R. Singh, D. McCarthy, M. Erhardt, J. P. Briand, M. Prato, K. Kostarelos and A. Bianco, *Angew. Chem., Int. Ed.*, 2004, **43**, 5242–5246.
- 5 N. W. S. Kam, Z. Liu and H. Dai, *J. Am. Chem. Soc.*, 2005, **127**, 12492–12493.
- 6 M. S. Strano, M. Zheng, A. Jagota, G. B. Onoa, D. A. Heller, P. W. Barone and M. L. Usrey, *Nano Lett.*, 2004, **4**, 543–550.
- 7 M. Zheng, A. Jagota, M. S. Strano, A. P. Santos, P. Barone, S. G. Chou, B. A. Diner, M. S. Dresselhaus, R. S. McLean, G. B. Onoa, G. G. Samsonidze, E. D. Semke, M. Usrey and D. J. Walls, *Science*, 2003, **302**, 1545–1548.
- 8 M. Zheng, A. Jagota, E. D. Semke, B. A. Diner, R. S. Mclean, S. R. Lustig, R. E. Richardson and N. G. Tassi, *Nat. Mater.*, 2003, **2**, 338–342.
- 9 H. Cathcart, V. Nicolosi, J. M. Hughes, W. J. Blau, J. M. Kelly, S. J. Quinn and J. N. Coleman, *J. Am. Chem. Soc.*, 2008, **130**, 12734–12744.
- 10 Y. Chen, H. Liu, T. Ye, J. Kim and C. Mao, *J. Am. Chem. Soc.*, 2007, **129**, 8696–8697.
- 11 S. Lyonnais, L. Goux-Capes, C. Escudé, D. Cote, A. Filoramo and J. P. Bourgoin, *Small*, 2008, **4**, 442–446.
- 12 X. Zhao and J. K. Johnson, *J. Am. Chem. Soc.*, 2007, **129**, 10438–10445.
- 13 (a) J. Chen, M. J. Dyer and M. F. Yu, *J. Am. Chem. Soc.*, 2001, **123**, 6201–6202; (b) G. Chambers, *Nano Lett.*, 2003, **3**, 843–846; (c) A. Ikeda, K. Hayashi, T. Konishi and J. Kikuchi, *Chem. Commun.*, 2004, 1334–1335.
- 14 C. V. Kumar and E. H. Asuncion, *J. Am. Chem. Soc.*, 1993, **115**, 8547–8553.
- 15 Y. Liu, L. Yu, Y. Chen, Y. L. Zhao and H. Yang, *J. Am. Chem. Soc.*, 2007, **129**, 10656–10657.
- 16 X. Peng, N. Komatsu, T. Kimura and A. Osuka, *J. Am. Chem. Soc.*, 2007, **129**, 15947–15953.
- 17 Y. Tomonari, H. Murakami and N. Nakashima, *Chem.-Eur. J.*, 2006, **12**, 4027–4034.
- 18 N. Nakayama-Ratchford, S. Bangsaruntip, X. Sun, K. Welsher and H. Dai, *J. Am. Chem. Soc.*, 2007, **129**, 2448–2449.
- 19 H. Wang, Y. Chen, X. Y. Li and Y. Liu, *Mol. Pharm.*, 2007, **4**, 189–198.
- 20 C. Journet and P. Bernier, *Appl. Phys. A: Mater. Sci. Process.*, 1998, **67**, 1.
- 21 J. Szejtli, *Chem. Rev.*, 1998, **98**, 1743–1753.
- 22 (a) Y. Liu, P. Liang, Y. Chen, Y. L. Zhao, F. Ding and A. Yu, *J. Phys. Chem. B*, 2005, **109**, 23739–23744; (b) Y. Liu, H. Wang, Y. Chen, C. F. Ke and M. Liu, *J. Am. Chem. Soc.*, 2005, **127**, 657–666; (c) Y. Liu, H. Wang, P. Liang and H. Y. Zhang, *Angew. Chem., Int. Ed.*, 2004, **43**, 2690–2694.